Int J Clin Exp Med 2015;8(3):4128-4133
www.ijcem.com /ISSN:1940-5901/IJCEM0003807

Original Article

The energy loss may predict rupture risks of anterior communicating aneurysms: a preliminary result

Peng Hu[1], Yi Qian[2], Chong-Joon Lee[2], Hong-Qi Zhang[1], Feng Ling[1]

[1]Department of Neurosurgery, Xuanwu Hospital, Capital Medical University, 45# Changchun Street, Beijing 100054, P.R. China; [2]Australia School of Advanced Medicine, Macquarie University, 2 Technology Place, Sydney 2109, Australia

Received November 13, 2014; Accepted January 31, 2015; Epub March 15, 2015; Published March 30, 2015

Abstract: Anterior communicating artery (ACoA) aneurysms are well documented to have a higher rupture risk compared with aneurysms at other locations. However, the risk predicting factors for these aneurysms still remain unclear due to the complex arteries geometries and flow patterns involved. The authors introduce a comprehensive method to quantitatively illustrate the development of ACoA aneurysms using a computational fluid dynamics (CFD) approach. Seven ACoA aneurysms, which included 2 ruptured and 5 unruptured aneurysms, were employed. Patient-specific whole anterior circulation geometries were segmented to simulate the real circumstances in vivo. The energy losses (EL) and flow architectures of these 7 aneurysms were evaluated using an algorithm modality. Overall, the 2 ruptured aneurysms, along with 1 unruptured aneurysm that was defined as highly likely to rupture due to ACoA location and a bleb sitting at the top of the dome, had a significantly larger EL and more complex and unstable flow architecture than the others. Two aneurysms had a negative value of EL indicating that the geometries with aneurysms of the anterior communicating complex (ACC) had a smaller loss of energy than the geometries without aneurysms. Despite a small sample size resulting in a low statistical significance, EL may serve as a development predictor of ACoA aneurysms.

Keywords: Anterior communicating artery aneurysm, aneurysm rupture, computational fluid dynamics, energy loss

Introduction

It is well known that aneurysmal subarachnoid hemorrhage can cause high morbidity and mortality even though numerous treatment modalities have been well developed [1]. On the other hand, the overall complication rate related to the treatment of unruptured intracranial aneurysms (UIAs) using either endovascular approach or open surgery was reported to be up to 7.1~13.7% [2]. Thus, the topic of whether an UIA should be treated or not remains controversial, especially for those with sizes less than 7 mm. A good understanding of the natural history of UIAs is regarded as a key solution for decision-making [2]. Although the designs of natural history studies have been evolving, it is still difficult to determine the rupture risk for a given aneurysm due to limited external validities of previous studies [1]. Being able to analyze individual hemodynamic parameters, CFD is used by many researchers to investigate any relationship between fluid dynamic characteristics and aneurysm rupture risks. Wall shear stress (WSS), oscillatory shear index (OSI), flow patterns within aneurysm dome, pressure loss (PL), and EL have been reported to potentially be able to predict the rupture risks of UIAs [3-6].

Anterior communicating artery aneurysms carry higher rupture risks than those at other locations [1]. The geometry and flow hemodynamic characteristics of this specific location, which possesses complex blood flow architecture determined by bilateral anterior cerebral arteries (ACAs), are different from those of other sites [7]. The number of studies reporting hemodynamic predictors of ACoA aneurysms is significantly less than for others such as side wall aneurysms. Moreover, there is still no quantitative analysis to predict ACoA aneurysm rupture so far. Meanwhile, EL, which measures the loss of energy due to blood flow passing through a given aneurysm, has been shown to

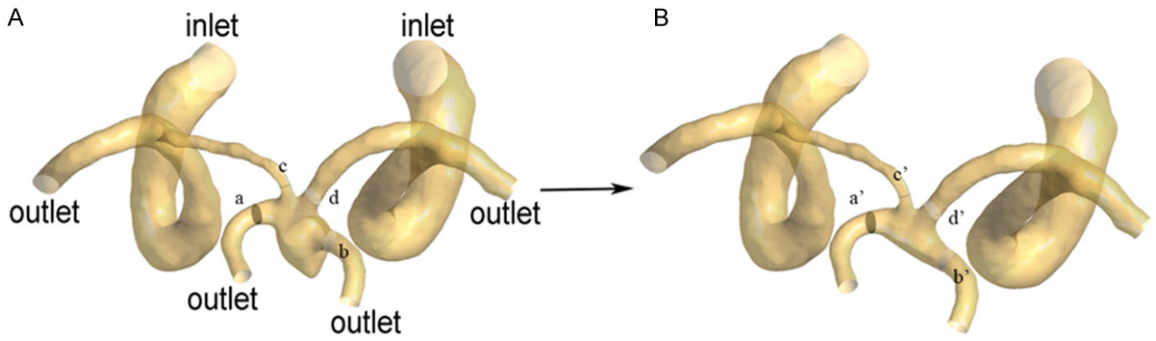

Figure 1. Illustration of algorithm involved in current study. A: The geometry with aneurysm. The planes built at bilateral anterior cerebral arteries were aimed to calculate the EL of ACC. B: The aneurysm was virtually removed. Note: The geometries of a case both with aneurysm and without aneurysm were kept exactly the same at all outlets and inlets. The planes built around the ACC were kept at exactly the same locations between geometries of a case.

Table 1. Summary of the sizes and EL of the 7 aneurysms

Aneurysms	Status	Size (mm)	Volume (mm^3)	EL (W)	EL_v (W/mm^3)*
1	Ruptured	7.1	7.40E-08	7.86879E-06	106.35
2	Ruptured	5.1	3.67E-08	3.69509E-06	100.71
3	Unruptured	3.9	2.05E-08	1.34371E-08	0.66
4	Unruptured	4.7	3.38E-08	-3.23471E-07	-9.56
5	Unruptured	6.6	1.27E-07	8.64819E-07	6.82
6	Unruptured	3.3	1.10E-08	-1.60147E-06	-145.75
7	Unruptured	3.8	3.32E-08	3.86299E-06	116.35

*EL_v is the EL standardized by volume of the aneurysm. EL: energy loss.

be one of the major factors involved in aneurysm initiation, growth, and rupture [4]. In current study, we developed a comprehensive method to quantitatively evaluate the EL of a given ACoA aneurysm based on a replication of the whole anterior circulation geometry, which was used to simulate the complex blood flow pattern at this specified site, and a more precise algorithm, which aims to eliminate confounding factors.

Materials and methods

This research was approved by the ethics committee of Macquarie University (approval no.: 2014005), and all participants provided informed written consent. All data collected under the current research project was patient-data blinded. Consequently, the sex and age were not available to be specified. Seven ACoA aneurysms including 2 ruptured aneurysms and 5 unruptured aneurysms from 7 patients were tested.

Numerical modeling methods

Computed tomography angiographies (CTA) with a slice thickness of 0.625 mm of these 7 patients were processed using the commercial software MIMICS 14.0 (Materialise Company, Belgium) to build patient-specific three-dimensional (3D) vascular geometries. More than 1 million mesh elements were generated using a commercial software package ICEM CFD 14.1 (ANSYS, Canonsburg, PA, USA). The number of elements was set based on our grid-independence analysis to obtain high quality simulation results [8]. In order to form a fully developed velocity profile, the inlets were extended to 20 times the size of the internal carotid arteries (ICAs) in upstream normal directions, and outlet domains were also extended in their respective downstream normal directions to 100 mesh layers (10 cm) for sufficient recovery of blood pressure. The governing equations employed in the current study were the Navier-Stokes equations. To simplify the calculations, the vessel walls were assumed to be rigid with no-slip condition, and the blood was assumed to be an incompressible, undergoing steady state, laminar Newtonian flow, with a constant density of 1050 kg/m^3 and a constant viscosity of 0.0035 Pa s. Because the patient-specific boundary conditions were not available, a mean mass flow rate of 0.00218 kg/s was presumed at inlets and an equal pressure was presumed at all outlets. The equations were solved using the

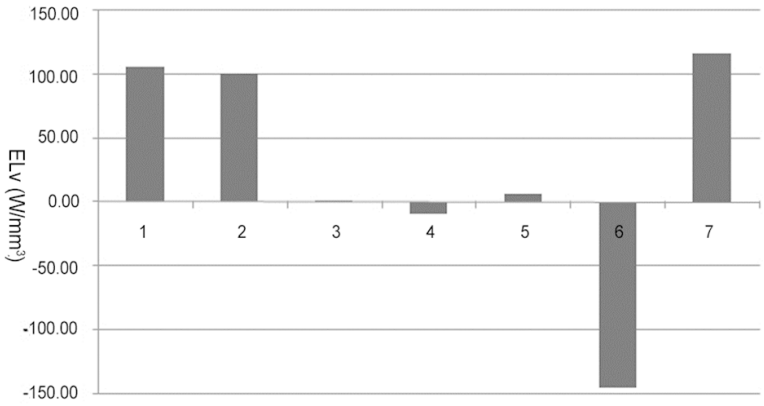

Figure 2. Bar graphic showing Elv's of the tested ACoA aneurysms. The ruptured aneurysms 1 and 2 and the unruptured aneurysm 7 with high rupture risk had significant larger EL magnitude than others.

CFX 14.1 solver package (ANSYS) on a HP Z800 workstation (Hewlett-Packard Company, Palo Alto, CA, USA).

Engergy loss

In order to precisely simulate the complex blood flow of ACoA, bilateral ICAs, middle cerebral arteries (MCAs), and ACAs, if any, were segmented (**Figure 1**). To calculate the EL caused purely by the aneurysm formation, we modelled a status of no aneurysm by virtually removing the aneurysm on MIMICS. Then EL of blood flow passing through an aneurysm could be evaluated by the EL differences of a given ACC between 'with aneurysm' status and 'no aneurysm' status (**Figure 1**). Mathematically, this can be expressed as: $\Delta EL = EL_{with\ aneurysm} - EL_{no\ aneurysm}$.

The energy (E) in general can be calculated based on the total pressure and the mass flow rate passing through a specific point: $E = V A ((1/2) \rho V^2 + P)$.

Where V presents the blood velocity, A is the area of the artery; ρ is the blood density, and P indicates the static blood pressure. Therefore, in case where there are multiple outlets and inlets, as is the case for ACoA aneurysms, the total EL of the ACC can be expressed as: $EL = \Sigma E_{inlets} - \Sigma E_{outlets}$.

Four cut-planes were set up around an aneurysm, which were defined as either inlet or outlet, were kept precisely at the same locations for both 'with aneurysm' and 'no aneurysm' statuses (**Figure 1**). Because the velocities and pressures might be altered by the change in geometries, the geometries of inlets and outlets remained untouched when the aneurysm was virtually removed to maintain uniformity between two models (**Figure 1**).

In order to compare the EL among different aneurysms, the magnitude of the EL was standardized by the volume of individual aneurysm, denoted ELv.

Results

The whole anterior geometries were segmented in all 7 patients. They were all featured as asymmetric ACAs including one patient (case 2) who had only one internal carotid artery. The details of these 7 tested aneurysms are summarized in **Table 1**. The sizes, which represented the largest diameters of the aneurysms on 3D geometries, of the two ruptured aneurysms were 7.1 mm and 5.1 mm respectively, while those of unruptured aneurysms ranged from 3.3 to 6.6 mm.

ELv of ruptured aneurysms had a significantly larger value than that of unruptured aneurysms except aneurysm 7. Two aneurysms had a negative value of ELv indicating that the geometries of the ACC with aneurysms had a smaller loss of energy than the geometries without aneurysms (**Table 1**; **Figure 2**). In other words, the initiation and growth of these two aneurysms decreased the EL of ACC.

Flow patterns in these seven aneurysms are represented in **Figure 3**. For the two ruptured aneurysms (aneurysm 1 and 2) and the 1 unruptured aneurysm with a large ELv magnitude (aneurysm 7), complex flow patterns with multiple vortices were noticed. In aneurysm 1, the blood flow direction of ipilateral A1 and A2 was reversed and the blood flow of the ipilateral A2 was conducted totally within the aneurysm, which eventually introduced multiple vortices formation. In aneurysm 2, most of the blood flow of ipilateral A2 was conducted to change flow direction within the aneurysm. Multiple vortices were formed within this aneurysm dome. In the unruptured aneurysm 7, entire ipilateral and part of the contralateral blood flow

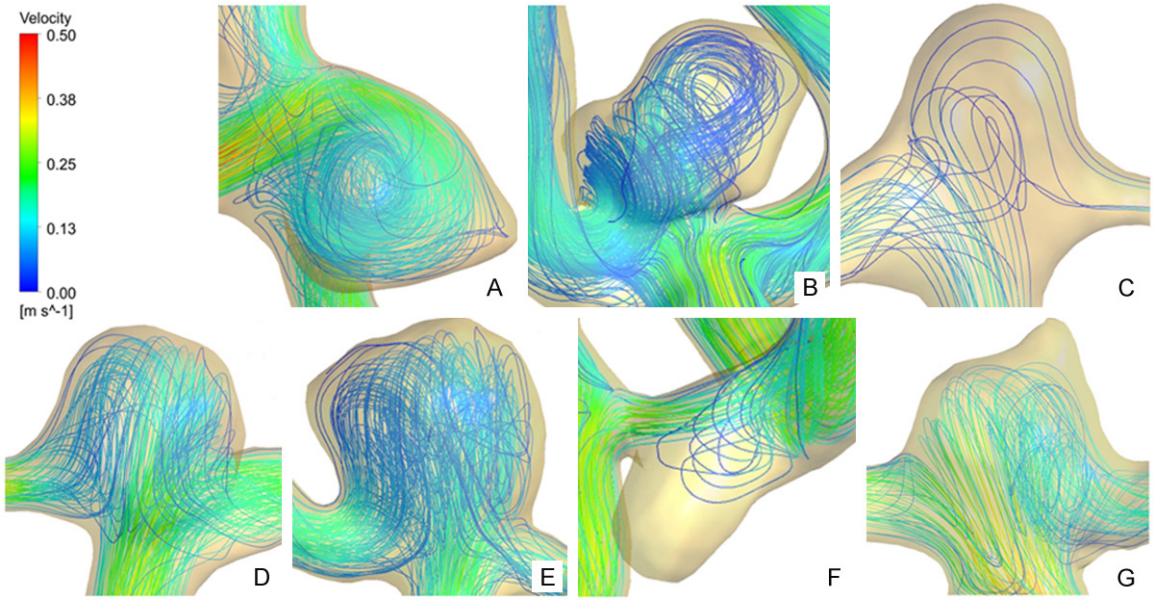

Figure 3. Simulated streamlines for the 7 patients. A: Streamlines of aneurysm 1 indicated the complex flow architecture with multiple vortices. The entire blood flow of ipilateral A2 was conducted within the aneurysm. B: Streamlines of aneurysm 2 indicated that almost entireblood flow of ipilateral A2 was conducted within the aneurysm and formed complex flow architecture with multiple vortices. C-F: Streamlines of aneurysms 3-6 individually. Aneurysms 3, 4, and 6 had simple flow patterns within aneurysm. Aneurysm 5 had small vortices passing through aneurysm dome. G: Streamlines of aneurysm 7. Bilateral blood flow of A2 were conducted within aneurysm dome and forming multiple complex vortices.

were conducted within the aneurysm and complex vortices were formed for each part. In aneurysm 5, a small part of the flow participated in forming vortices and ELv for this aneurysm turned out to be larger than for the other three unruptured aneurysms which exhibited only simple flow patterns.

Discussion

Aneurysms of different locations carry different rupture risks [1, 2]. Even small ACoA aneurysms (those with sizes smaller than 7 mm) were shown to be more likely to rupture compared with aneurysms at other locations [9]. It was addressed that complex geometry diversities and flow patterns might play an important role in the process of ACoA aneurysm rupture [10, 11].

The blood flow passing through the ACoA is determined by bilateral anterior cerebral arteries. Symmetric anterior cerebral arteries may yield a zero net mass flow rate through the ACoA, however, cross flow may still exist producing high WSS which may contribute to aneurysm initiation [12]. It was argued that asymmetric bilateral anterior cerebral arteries were related to high odds ratio of presence and development of ACoA aneurysms [13].

The application of the EL for quantitatively estimating intracranial aneurysm rupture risk was initially advocated by Qian et al [4]. Theoretically, blood flow may lose energy when it passes through an aneurysm due to flow separation, forming vortices, flow direction alternation, and interaction with aneurysm walls [4]. The EL was introduced to quantitatively calculate this energy loss and was shown to be able to predict the rupture risk of side wall aneurysms [4, 14]. However, this quantitative parameter has not been applied to ACoA aneurysms due to their complex geometries and flow patterns with multiple inlets and outlets. In this study, we built bilateral ICA geometries so as to distribute flow profiles as determined by geometries of the ICA, MCA, and ACA themselves, which might simulate the context in vivo. The ELv in the two ruptured ACoA aneurysms were significantly higher than others except aneurysm 7. However, the aneurysm 7 was defined as unruptured due to the patient having no subarachnoid hemorrhage before the aneurysm was disclosed, which did not necessarily mean that the rupture risk of this aneurysm was not high.

Moreover, this aneurysm will certainly be recognized as high rupture risk aneurysm, which was located at ACoA and featured a bleb at the top of its dome, according to previous large multiple-center prospective cohort studies [1, 2]. All these 3 aneurysms with high ELv have intra-aneurysm complex flow patterns with multiple vortices which was reported to be related to high aneurysm rupture risks [15]. For the aneurysms with negative ELv, the negative value might illustrate that the formation of these two ACoA aneurysms was initiated to reduce the energy loss of these ACCs. At the initiation stage, the flow patterns within the aneurysms remained simple. During the growth of the ACoA aneurysms, the flow patterns within the aneurysms changed to be more complex and consequently resulted in more loss of energy. In summary, the ELv may reflect rupture risks of ACoA aneurysms.

This study contains limitations. A small number of patients cannot statistically address a powerful conclusion. On the other hand, the analysis was not based on patient-specific boundary conditions due to a retrospective study design. However, the authors established a comprehensive method to calculate the ELv which could be able to quantitatively predict rupture risks of ACoA aneurysms, which are characterized by more complex fluid dynamic patterns than other aneurysms. Based on this preliminary study, the ELv will be applied to our ongoing multiple-center prospective aneurysm rupture risk study.

Conclusions

The ELs of ACoA aneurysms can be quantitatively evaluated by comprehensive CFD processing modalities. The magnitude of ELv may delineate the flow architectures within ACoA aneurysms and eventually predict the rupture risks of ACoA aneurysms. However, a large cohort is needed to reach a sufficient statistic power.

Acknowledgements

Doctors Peng Hu and Hong-Qi Zhang are financially supported by Capital Development Funds of Medical Science with a grant number of "2011-1001-01". The authors would like to thank David Verrelli for his laguage editing. Otherwise, the authors have no any personal or institutional financial interest in drugs, materials, or devices.

Disclosure of conflict of interest

None.

Address correspondence to: Hong-Qi Zhang, Department of Neurosurgery, Xuanwu Hospital, Capital Medical University, 45# Changchun Street, Beijing 100054, P.R. China. Tel: +86 10 83198899; Fax: +86 10 83198136; E-mail: hongqizhang2014@163.com

References

[1] Morita A, Kirino T, Hashi K, Aoki N, Fukuhara S, Hashimoto N, Nakayama T, Sakai M, Teramoto A, Tominari S and Yoshimoto T. The natural course of unruptured cerebral aneurysms in a Japanese cohort. N Engl J Med 2012; 366: 2474-2482.

[2] Wiebers DO, Whisnant JP, Huston J 3rd, Meissner I, Brown RD Jr, Piepgras DG, Forbes GS, Thielen K, Nichols D, O'Fallon WM, Peacock J, Jaeger L, Kassell NF, Kongable-Beckman GL and Torner JC. Unruptured intracranial aneurysms: natural history, clinical outcome, and risks of surgical and endovascular treatment. Lancet 2003; 362: 103-110.

[3] Cebral JR, Mut F, Weir J and Putman C. Quantitative characterization of the hemodynamic environment in ruptured and unruptured brain aneurysms. AJNR Am J Neuroradiol 2011; 32: 145-151.

[4] Qian Y, Takao H, Umezu M and Murayama Y. Risk analysis of unruptured aneurysms using computational fluid dynamics technology: preliminary results. AJNR Am J Neuroradiol 2011; 32: 1948-1955.

[5] Xiang J, Natarajan SK, Tremmel M, Ma D, Mocco J, Hopkins LN, Siddiqui AH, Levy EI and Meng H. Hemodynamic-morphologic discriminants for intracranial aneurysm rupture. Stroke 2011; 42: 144-152.

[6] Takao H, Murayama Y, Otsuka S, Qian Y, Mohamed A, Masuda S, Yamamoto M and Abe T. Hemodynamic differences between unruptured and ruptured intracranial aneurysms during observation. Stroke 2012; 43: 1436-1439.

[7] Castro MA, Putman CM and Cebral JR. Patient-specific computational fluid dynamics modeling of anterior communicating artery aneurysms: a study of the sensitivity of intra-aneurysmal flow patterns to flow conditions in the carotid arteries. AJNR Am J Neuroradiol 2006; 27: 2061-2068.

[8] Qian Y, Liu JL, Itatani K, Miyaji K and Umezu M. Computational hemodynamic analysis in congenital heart disease: simulation of the Norwood procedure. Ann Biomed Eng 2010; 38: 2302-2313.

[9] Bijlenga P, Ebeling C, Jaegersberg M, Summers P, Rogers A, Waterworth A, Iavindrasana J, Macho J, Pereira VM, Bukovics P, Vivas E, Sturkenboom MC, Wright J, Friedrich CM, Frangi A, Byrne J, Schaller K and Rufenacht D. Risk of rupture of small anterior communicating artery aneurysms is similar to posterior circulation aneurysms. Stroke 2013; 44: 3018-3026.

[10] Mira JM, Costa FA, Horta BL and Fabiao OM. Risk of rupture in unruptured anterior communicating artery aneurysms: meta-analysis of natural history studies. Surg Neurol 2006; 66 Suppl 3: S12-19.

[11] Castro MA, Putman CM, Sheridan MJ and Cebral JR. Hemodynamic patterns of anterior communicating artery aneurysms: a possible association with rupture. AJNR Am J Neuroradiol 2009; 30: 297-302.

[12] Jou LD, Lee DH and Mawad ME. Cross-flow at the anterior communicating artery and its implication in cerebral aneurysm formation. J Biomech 2010; 43: 2189-2195.

[13] Tarulli E and Fox AJ. Potent risk factor for aneurysm formation: termination aneurysms of the anterior communicating artery and detection of A1 vessel asymmetry by flow dilution. AJNR Am J Neuroradiol 2010; 31: 1186-1191.

[14] Liu J, Xiang J, Zhang Y, Wang Y, Li H, Meng H and Yang X. Morphologic and hemodynamic analysis of paraclinoid aneurysms: ruptured versus unruptured. J Neurointerv Surg 2013; 6: 658-63.

[15] Cebral JR, Castro MA, Burgess JE, Pergolizzi RS, Sheridan MJ and Putman CM. Characterization of cerebral aneurysms for assessing risk of rupture by using patient-specific computational hemodynamics models. AJNR Am J Neuroradiol 2005; 26: 2550-2559.